A Robust Timing Recovery Algorithm for Faster-than-Nyquist Digital Multi-band System

Hao Deng[1], Wanzhen Guo[1], Yi Cai[2], and Jian Zhao[1]
[1]*School of Electronic and Information Engineering, South China University of Technology, Guangzhou, China*
[2]*Soochow University, Suzhou, Jiangsu, China*
e-mail address: zhaojian@scut.edu.cn

Abstract: We propose a novel timing-recovery algorithm (TRA) for faster-than-Nyquist digital-multi-band systems, and experimentally demonstrate that the proposed TRA works for different compression ratios and outperforms conventional TRAs in dispersion and DGD tolerance and convergence speed. © 2024 The Author(s)

1. Introduction

Faster-than-Nyquist (FTN) technology compresses the signal bandwidth lower than the baud rate and has the potential to reduce the interval between channels/subbands to increase the spectral efficiency or achieve a higher baud rate under device bandwidth limitation [1-2]. Although FTN filtering induces inter-symbol interference (ISI), it can be compensated by maximum likelihood sequence estimation (MLSE) or the BCJR algorithm [2].

On the other hand, timing recovery (TR) is an essential element to synchronize the clocks between the transmitter and receiver. However, the compressed bandwidth of the FTN signal makes conventional Gardner or Godard algorithms fail [3]. A square-Gardner (sGardner) method was proposed to overcome the failure of TRAs under small roll-off factors [4] and could be applied to FTN. However, this method does not work when the differential group delay (DGD) is equal to half of the symbol period. In [5], a joint timing recovery and equalization method was proposed to avoid the singularity condition by performing equalization first. This inevitably increases the feedback loop delay and limits the locking capability. Recently, we proposed a pilot-aided TRA for offset-quadrature-amplitude-modulation digital multi-band (OQAM-DMB) systems [6]. However, additional investigation shows that this algorithm cannot be applied to the FTN-DMB system.

In this paper, we modify the method in [6] to adapt to the FTN-DMB system and experimentally verify its effectiveness under different compression ratios. It is demonstrated that the proposed TRA exhibits a faster convergence speed and more robust tolerance to residual chromatic dispersion (rCD) than the sGardner method. It is also insensitive to DGD even when it is equal to half of the symbol period.

2. Principle

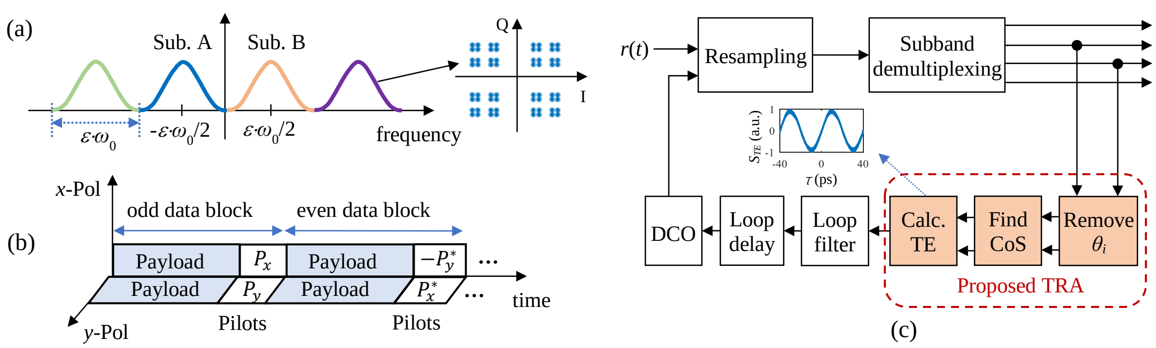

Fig. 1. (a) Spectral diagram of a 4-subband FTN-DMB signal, where ε≤1 is the compression ratio. Inset: An example of constellation for QPSK-FTN. (b) Design of pilots in both subband A and subband B. (c) Principle of the digital phase-lock loop using the proposed TRA.

Fig. 1(a) depicts the spectral diagram of a 4-subband FTN-DMB signal. Here, $\omega_0/(2\pi)$ is the baud rate per subband. For FTN, we adopt Gaussian-shaped spectrum with truncated spectral tails and optimized 3-dB bandwidth for a given compression ratio ε, $\varepsilon\leq1$. Inset of Fig. 1(a) depicts the constellation of the QPSK-FTN signal, where ISI exists but can be compensated by MLSE or BCJR at the receiver. Because FTN has a bandwidth narrower than the baud rate, conventional TRAs such as Gardner and Godard algorithms fail. The proposed TRA is based on the pilots in subbands A and B as designed in Fig. 1(b), where the two subbands have the same pilots. This design ensures that the position of pilots in the received signal stream can always be identified via the symmetry property of the correlation function of pilots regardless of the state of polarization (SOP), DGD, residual frequency offset (RFO) and rCD [6]. Note that these pilots can be re-used for carrier phase recovery and polarization demultiplexing. Fig. 1(c) shows the principle of the digital phase-lock loop (DPLL) using the proposed TRA to correct the timing error (TE). The DPLL works on a block-by-block basis. In each loop iteration, the received signal block is firstly demultiplexed. When there is a TE τ, the demultiplexed x- and y-polarization signals for subbands A and B in the i^{th} loop iteration can be derived as:

$$\begin{bmatrix} s_{A,x,i}(t) \\ s_{A,y,i}(t) \end{bmatrix} = h_A(t) \otimes \sum_{n=(i-1)N}^{iN-1} \begin{bmatrix} s_{A,x}(n) \\ s_{A,y}(n) \end{bmatrix} \cdot h(t-nT-\tau)\cdot \exp(j\varepsilon\omega_0\tau/2 + j\theta_i + j\varphi(t)) \tag{1-1}$$

$$\begin{bmatrix} s_{B,x,i}(t) \\ s_{B,y,i}(t) \end{bmatrix} = h_B(t) \otimes \sum_{n=(i-1)N}^{iN-1} \begin{bmatrix} s_{B,x}(n) \\ s_{B,y}(n) \end{bmatrix} \cdot h(t-nT-\tau)\cdot \exp(-j\varepsilon\omega_0\tau/2 - j\theta_i + j\varphi(t)) \tag{1-2}$$

where $s_{A/B,x/y}(n)$ are the transmitted symbols in x/y polarization in subband A/B. $h_{A/B}(t)$ are the Jones matrices. $h(\cdot)$ is the FTN signal pulse. N is the number of symbols in one iteration and T is the symbol period of a subband. $\varphi(t)=\varphi_p(t)+\beta_2L(\varepsilon\omega_0)^2/8+\Delta\omega(t-\tau)$, where $\varphi_p(t)$, β_2L and $\Delta\omega$ are the phase noise, rCD and RFO, respectively. $\theta_i=\varepsilon\cdot\omega_0\cdot(i-1)NT$.

In contrast to conventional OQAM-DMB, the subband interval of FTN-DMB is not equal to the baud rate (i. e. $\varepsilon\cdot\omega_0T\neq 2k\pi$, k is an arbitrary integer). Therefore, there is a residual phase θ_i in Eq. (1) for different DPLL iterations, which will affect the TE calculation. Therefore, in FTN, we should remove the residual phase θ_i (=$\varepsilon\cdot\omega_0\cdot(i-1)NT$) by:

$$s_{\text{modified},A,x/y,i}(t) = s_{A,x/y,i}(t)\cdot\exp(-j\theta_i),\; s_{\text{modified},B,x/y,i}(t) = s_{B,x/y,i}(t)\cdot\exp(j\theta_i) \tag{2}$$

Then we extract the pilot symbols from $s_{\text{modified},A,x/y,i}$ and $s_{\text{modified},B,x/y,i}$, and perform:

$$A_t = A_{x,odd}\cdot A'_{y,even} - A_{x,even}\cdot A'_{y,odd} \qquad B_t = B_{x,odd}\cdot B'_{y,even} - B_{x,even}\cdot B'_{y,odd} \tag{3}$$

where $A_{x,odd}$, $A_{x,even}$, $A_{y,odd}$, $A_{y,even}$, $B_{x,odd}$, $B_{x,even}$, $B_{y,odd}$, $B_{y,even}$ are the odd and even pilot waveforms of x- and y-polarizations for subbands A and B. $(\cdot)'$ represents the flipped waveform about the center of symmetry (CoS), which can be obtained using the correlation function of the pilots. The TE can be obtained by:

$$S_{TE} = \mathrm{Im}[(A_t + A'_t)\cdot(B_t + B'_t)^*] \tag{4}$$

This TE is then fed back to digitally resample the signal or to adjust the clock sampling phase of the ADCs.

3. Experimental Setup and Results

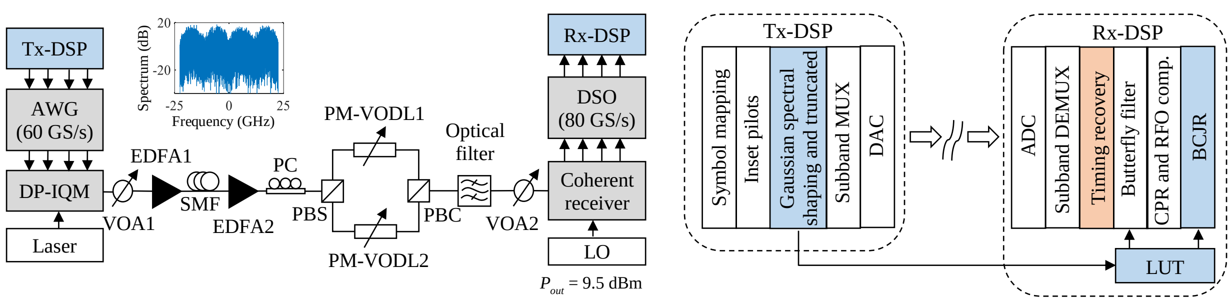

Fig. 2. Experimental setup and the DSP flows at the transmitter and receiver. Inset: the spectrum of generated FTN-DMB. AWG: arbitrary waveform generator; DP-IQM: dual-polarization IQ modulator; VOA: variable optical attenuator; SMF: single mode fiber; PC: polarization controller; PM-VODL: polarization-maintaining variable optical delay line; PBS/PBC: polarization beam splitter/combiner; DSO: digital storage oscilloscope.

Fig. 2 shows the experimental setup of the FTN-DMB system with DP-QPSK format. A Gaussian-shaped digital filter was used to create the FTN spectrum. For each ε, the 3-dB bandwidth of the Gaussian spectrum was optimized to minimize the bit error rate (BER). To facilitate decoding at the receiver, a look-up table (LUT) was used to store the relationship between ISI at a symbol and the symbols around it (3 in this paper). Four subbands were multiplexed and pilot symbols were inserted into subbands A and B at a ratio of 1/32. The pilots P_x and P_y as depicted in Fig. 1(b) were set to be 1+j and 1-j, respectively. Inset shows the spectrum of the generated FTN-DMB signal for ε=0.9. The signal was then uploaded into a 20GHz AWG operating at 60 GS/s and modulated a CW light via a DP-IQM. In the optical link, a piece of SMF was added to investigate the influence of rCD while DGD was emulated by two PM-VODLs. The OSNR was set as 28 dB. The power of the signal into the coherent receiver was -7 dBm. In the receiver DSP, TE was first added to emulate different clock frequency offsets (CFO) and initial sampling phase offsets. The signal with TE was demultiplexed into subbands. Subbands A and B were used to calculate the TE which was fed back to control the digital oscillator. N in Eq. (1) was set as 128. A delay of 10.24 ns was added to emulate the DPLL loop delay. The following DSP after TR included butterfly filtering and phase estimation. Finally, each FTN signal was decoded using BCJR based on the LUT and the BER was measured after the DPLL had been locked.

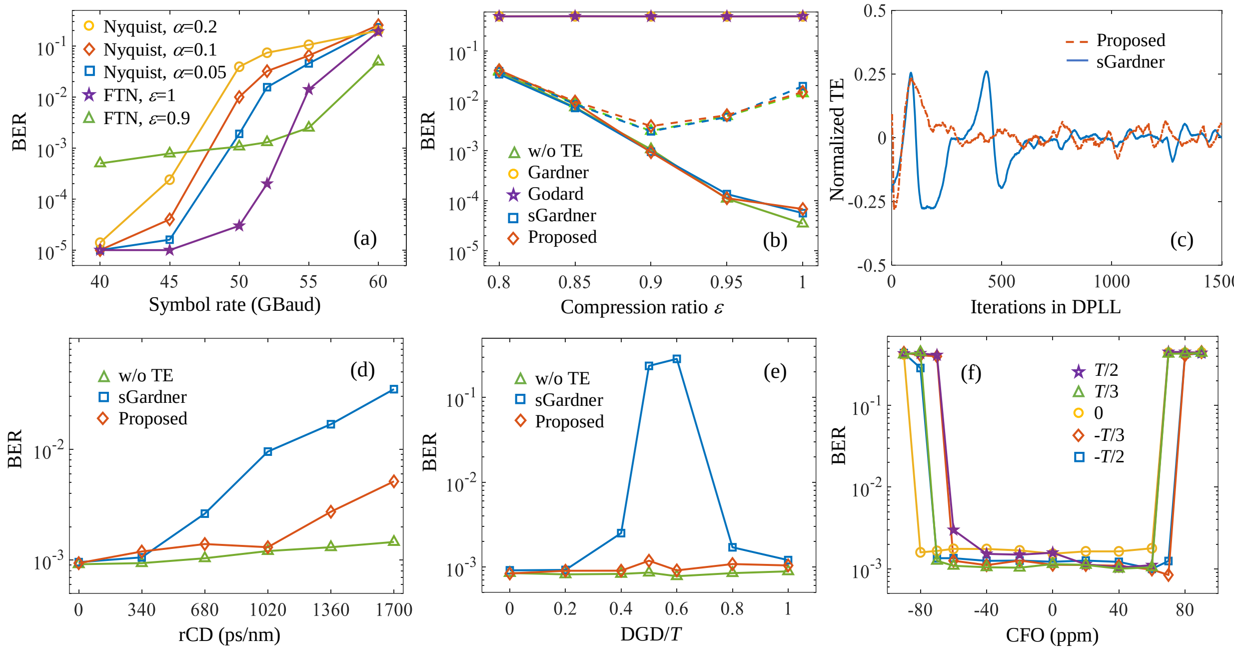

Fig. 3. (a) BER versus baud rate for Nyquist-DMB with different roll-off α and FTN-DMB with different ε. (b) BER versus ε. The solid and dashed lines represent 50 GBaud and 55 GBaud, respectively. (c) The convergence curves of the DPLL. (d) BER versus rCD. (e) BER versus DGD. (f) BER versus CFO under different initial sampling phases. In (b)-(e), the CFO is 20 ppm. In (c)-(f), ε=0.9 and the symbol rate is 50 GBaud.

We first investigate the performance of conventional Nyquist-DMB and FTN-DMB without TE, as shown in Fig. 3(a). For Nyquist-DMB, it is seen that the performance is excellent at lower symbol rate but degrades significantly due to device bandwidth limitation as the symbol rate increases, especially when the roll-off factor is large. On the other hand, FTN-DMB with ε=1 exhibits better performance than conventional Nyquist-DMB at all symbol rates. For ε=0.9, a penalty is observed at lower symbol rates due to ISI but higher symbol rates can be achieved. Next, we investigate the performance of TRAs for FTN-DMB, as shown in Fig. 3(b). It is seen that ε=1 is the best at 50 GBaud while ε=0.9 is optimal at 55 GBaud to balance the distortion induced by bandwidth limitation and FTN-induced ISI. For all ε, the proposed method and sGardner algorithm achieve negligible penalties while the Gardner and Godard algorithms fail. Fig. 3(c) shows the convergence curves of the DPLL. It is seen that the proposed method converges faster than the sGardner algorithm and the DPLL can be locked after 250 iterations. We then compare the proposed TRA and sGardner in terms of the rCD and DGD tolerance, as shown in Fig. 3(d)-(e). It is seen that the proposed TRA doubles the rCD tolerance and overcomes the shortcoming of the sGardner algorithm that fails when DGD is equal to T/2. In addition, the proposed TRA tolerates ±60 ppm CFO for all initial sampling phase offsets, as shown in Fig. 3(f).

4. Conclusions

We have proposed and experimentally demonstrated a novel pilot-aided TRA for FTN-DMB. 50GBaud experiments show that the proposed TRA works properly for different compression ratios in FTN-DMB while conventional Gardner and Godard algorithms fail. Compared to sGardner, the proposed TRA is more robust to rCD and DGD and have a faster convergence speed. This work was supported by the National Key Research and Development Program of China (2022YFB2903000) and National Natural Science Foundation of China (61971199).

5. References

[1] J. E. Mazo, "Faster-than-Nyquist signaling," The Bell System Technical Journal, vol. 54, no. 8, pp. 1451-1462, 1975.
[2] Y. Cai et al., "Combined symbol-pattern-dependent adaptive equalization and sequence detection for coherent optical fiber communications," JLT, vol. 40, no. 5, pp. 1320-1329, 2022.
[3] F. Gardner, "A BPSK/QPSK timing-error detector for sampled receivers," IEEE TCom, vol. 34, no. 5, pp. 423-429, 1986.
[4] M. Yan et al., "Digital clock recovery algorithm for Nyquist signal," OFC, paper OTu2I.7, 2013.
[5] J. You et al., "Joint timing recovery and adaptive equalization based on training sequences for PM-16QAM faster-than-Nyquist WDM systems," OE, vol. 31, no. 20, pp. 33421-33434, 2023.
[6] W. Guo et al., "A novel pilot-aided timing recovery algorithm with high tolerance to impairments for OQAM-based digital multi-band systems," JLT, vol. 41, no. 11, pp. 3539-3550, 2023.